Magneto-optical studies of screened excitons in GaAs/$Al_xGa_{1-x}As$ modulation-doped quantum wells

A. B. Henriques
Instituto de Física da Universidade de São Paulo, Caixa Postal 20516, 01498 São Paulo, Brazil

E. T. R. Chidley and R. J. Nicholas
Clarendon Laboratory, Oxford OX1 3PU, United Kingdom

P. Dawson
The University of Manchester Institute of Science and Technology, Manchester, United Kingdom

C. T. Foxon
Physics Department, Nottingham University, United Kingdom

(Received 13 January 1992; revised manuscript received 11 March 1992)

Asymmetric GaAs/$Al_xGa_{1-x}As$ quantum wells were studied by photoconductivity and photoluminescence in magnetic fields up to 15 T. The sample chosen had only one occupied electric subband, with a high density of 8.2×10^{12} cm^{-2}, which allowed a study of the empty $E2$-$H1$ transitions by photoconductivity. This showed that there was a small but finite binding energy of 1.5 ± 0.5 meV for the $1s$ state, which increased very rapidly at high fields in agreement with theory, due to the changing effects of the screening on the exciton. No evidence was seen for excitonic contributions to any higher-Landau-level transitions. Photoluminescence was used to study the $E1$-$H1$ transition, which was shown to be due to free-carrier recombination.

Modulation-doped quantum wells (MDQW's) provide nearly ideal systems for the study of many-body physical phenomena, such as band-gap renormalization (BGR) and Moss-Burstein shift between absorption and emission,[1] Fermi-edge singularities,[2] magneto-optical oscillatory phenomena,[3–5] and exciton screening at high densities.[6] The binding energies of screened excitons, which are formed between empty electric and hole subbands, have already been estimated for a 250-Å MDQW, with a carrier density of 7.6×10^{11} cm^{-2}, from magnetophotoluminescence excitation spectra, whereby the two-dimensional approximation was employed to fit the experimental data, with the exciton binding energy as an adjustable parameter.[7] Recently, a model for the screened exciton has been proposed,[8] which allows one to calculate the screened exciton binding energy with the inclusion of the nonzero thickness of the screening charge, and which requires no adjustable parameters, showing that the exciton binding energy is strongly dependent on the QW width and doping level, and this model predicts correctly the exciton binding energy for a sample with the same parameters as the one studied in Ref. 7. Moreover, this model allows calculation of the exciton binding-energy dependence on the intensity of a magnetic field applied perpendicular to the interfaces, and in the present work such a theoretical dependence is tested experimentally.

We report measurements of magnetoresistance, photoluminescence (PL), and photoconductivity (PC) of 150-Å GaAs/$Al_xGa_{1-x}As$ MDQW's at 4.2 K in magnetic fields up to 15 T. The sample chosen had only one occupied subband. The screened exciton binding energy was deduced from the magnetophotoconductivity spectra, whereby the finite thickness of the screening charge was included in the analysis in the frame of Ref. 8, confirming that screening reduces the binding energy, but does not quench the exciton formation, in agreement with Ref. 7. The magnetic-field dependence of the exciton binding energy was studied, and it is well reproduced by the theory, which provides new support for the screened exciton model described in Ref. 8. Photoluminescence was used to study the $E1$-$H1$ recombination, which showed no excitonic effects. This confirms the earlier conclusion[7] that phase-space filling is an efficient mechanism of quenching of the exciton formation.

I. EXPERIMENT

The samples were grown by molecular-beam epitaxy at Philips Research Laboratories. Sample 1 comprises a 0.5-μm GaAs buffer on a (100) GaAs substrate, followed by 0.5 μm of a [GaAs (6 monolayers)]-[AlAs (3 monolayers)] superlattice, forming one side of the barrier of the quantum well, 150 Å of a GaAs quantum well, a 22-Å spacer of undoped $Al_{0.25}Ga_{0.75}As$, then 400 Å of 1.5×10^{18} cm^{-3} Si-doped $Al_{0.25}Ga_{0.75}As$, and finally a 100-Å GaAs capping layer. The structure so formed is hence asymmetric with respect to doping and also with respect to the barriers on either side of the GaAs quantum well.

Experiments were carried out in a superconducting magnet. The sample was placed in He exchange gas in an insert in thermal contact with liquid He at 4.2 K. Light was conveyed to the sample, and collected from the sam-

ple, by a quartz optical fiber bundle. All experiments were done in the Faraday configuration. Standard lock-in techniques were employed in the detection. The photoconductivity and Shubnikov–de Haas measurements were made using a four-contact geometry; the sample itself was approximately square, with contacts in the corners. The photoconductivity was done in constant current mode, employing currents of ~ 80 μA. A filament lamp was used as the excitation source for photoconductivity. The light was dispersed by a 1-m Spex monochromator equipped with a 1.6-nm/mm grating. Photoluminescence was excited by the 488-nm line of an Ar-ion laser, and detected by a GaAs photomultiplier.

The density of confined electrons was monitored under the experimental conditions by Shubnikov–de Haas (SdH) measurements. Good SdH traces were obtained only when the sample was in darkness or weakly illuminated, as for photoconductivity, with oscillations clearly visible down to around 1 T. Under laser illumination, the Shubnikov–de Haas oscillations became progressively less resolved as the laser power was increased, disappearing into a positive background of magnetoresistance. Under the experimental conditions for photoluminescence, the oscillations are barely discernable, though they may be seen in the second derivative of the signal. In complete darkness, we obtain a carrier density of $n_s = 5.7 \times 10^{11}$ cm^{-2}, in good agreement with previously published data[9] on this sample, which also report a 4.2-K maximum mobility of 150 000 cm^2/V s. Under the illumination conditions of PC and PL experiments, n_s increases to 8.2×10^{11} cm^{-2} and 9.3×10^{11} cm^{-2}, respectively. This allows the position of the Fermi level relative to the bottom of the $E1$ subband, $F = \pi\hbar^2 n_s / m^*$, to be calculated, where $m^* = 0.0735 m_0$ is the electron effective mass, measured by far-infrared transmission[10] for this sample. This gives $F = 26$–30 meV, implying that only the fundamental $E1$ subband is occupied under the experimental conditions.

A second sample (No. 2) was also studied by magnetotransport, photoluminescence, and photoconductivity in the 0–15-T field range. This sample is identical to No. 1, apart from the inverted interface, which in sample 2 is bulk $Al_{0.33}Ga_{0.67}As$ instead of the Al-As superlattice. For this sample, however, the Shubnikov–de Haas oscillations were not so well defined as for sample 1. PC spectra were also less well resolved, although the same general features as for sample 1 could be seen. However, since resolution was poorer for sample 2, no extensive study was made. This illustrates the point that growing the quantum well on a short-period superlattice does, indeed, reduce the scattering at the inverted interface, thus improving the optical and electrical quality of the sample.[11]

II. INTERBAND TRANSITIONS IN ZERO MAGNETIC FIELD

Figure 1 shows the zero-field photoconductivity and photoluminescence spectra. The PL shows two transitions which it is assumed are associated with the bulk GaAs—one unresolved free electron to neutral carbon acceptor and corresponding donor-acceptor pair transition (these are partially resolved under excitation at 1.727 eV) , and a bulk GaAs exciton. A broadband peaking at 1.45 eV was also detected and is attributed to the quartz fiber bundle.

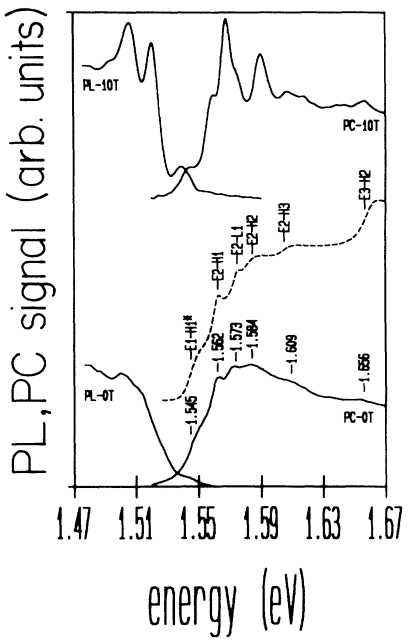

FIG. 1. PC and PL spectra (solid curves) at $B = 0$ and $B = 10$ T. The dashed curve is the calculated absorption spectrum at $B = 0$ T; the adjustable parameters were $c = 1.9$ and a BGR of -13.7 meV. The energy position of the Moss-Burstein edge (marked by an asterisk) and excitonic transitions are indicated.

The energy offset between the PL and the onset of the PC response (~ 30 meV) occurs due to the blocking of absorption up to the Fermi wave vector—the Moss-Burstein shift. At high fields, when the magnetic quantum limit is approached, such an energy shift is partially quenched. This is illustrated in Fig. 1, which shows that at 10 T there is an overlap between the PL and PC spectra; absorption becomes permitted in the $N = 1$ Landau-level state just below the Fermi energy through finite-temperature effects. The overlapping transitions in Fig. 1 correspond to an $E1$-$H1$ Landau-level transition, showing a Stokes' shift of ~ 3 meV.

It is to be noted that, apart from the substrate-related emissions, the zero-field PL spectrum does not present any sharp features in the spectral region of QW luminescence, indicating the absence of strong excitonic features. Since the PL spectrum is expected to show transitions originating from the $E1$ subband, we interpret this result as being due to the phase-space filling (PSF) mechanism of exciton quenching.[1] In contrast, the zero-field PC spectrum displays sharp features, such as peaks at 1.562 and 1.573 eV, which are a clear indication of exciton formation between hole and empty electronic subbands. These excitons are transitions to higher-lying states and are also expected to be described by a binding energy which is reduced from the undoped value on account of the screening charge, present in the $E1$ subband.

In order to identify the features which appear in the zero-field spectra, the energies, and oscillator strengths, of the intersubband optical transitions were calculated in the self-consistent Hartree approximation as described in Ref. 12. In these calculations, the nominal sample parameters and carrier density in the QW under the conditions of the PC experiment ($n_s = 8.2 \times 10^{11}$ cm^{-2}) were used. The dielectric constant was taken to be 12.6 throughout the structure, and m^* as $(0.0735 + 0.08x)m_0$. The band-edge transverse $H1$ and $L1$ hole masses were taken as $0.25m_0$ (Refs. 12 and 13) and $0.21m_0$,[14] respectively, and the $H1$ and $L1$ hole masses along the growth direction were taken as $(0.38 + 0.1x)m_0$ and $(0.087 + 0.06x)m_0$, respectively. The conduction-band offset was taken to be $0.65\Delta E_g$, where $\Delta E_g = 1.247x$ eV, and the bulk GaAs band gap is 1.519 eV. In all expressions, x denotes the local aluminum molar fraction. We have also calculated the zero-field binding energies of the screened $E2$-$H1$ and $E2$-$L1$ transitions by the method of Ref. 8. Following Ref. 15, the energy of the Burstein-Moss-shifted $E1$-$H1^*$ absorption (the asterisk meaning a direct transition at the Fermi wave vector) was calculated by adding $(1 + m^*/m_{H1})F$ to the $E1$-$H1$ Γ-point transition energy, where m_{H1} is the transverse $H1$ effective mass and $F = 27$ meV as for the PC experiment.

With the calculated intersubband transition energies and oscillator strengths, the theoretical absorption spectrum was generated, and is shown in Fig. 1 by the dashed curve. In this procedure, we followed the prescription of Ref. 16: each transition is described by a smooth step function and an excitonic satellite—a Lorentzian of half width cN_eN_h(meV), where c is of the order of unity and N_e, N_h are the electron and subband indexes for a given transition. To obtain agreement between the measured and the calculated spectra, it was necessary to add a band-gap renormalization energy to the bulk GaAs band gap (see Table I).

The theoretical absorption spectrum in Fig. 1 was obtained by adding a constant BGR of -13.7 meV to the calculated transition energies, giving a reasonable agreement with the experiment. The only other adjustable parameter is c, which describes the smoothness of the step in the combined density of states and the half width of the exciton peaks. The fixed value of BGR for intersubband transitions involving both filled and empty electronic subbands supports early BGR measurements,[6] which report a BGR of -18 meV for either filled or empty subbands (for a QW of width $L_z = 130$ Å and a carrier density of $n_s = 7 \times 10^{11}$ cm^{-2}), but disagrees with more recent results,[7] which find a BGR of -10 meV for the $E1$-$H1$ energy gap, but only -3 meV for $E2$-$H1$ (for $L_z = 250$ Å and $n_s = 7.6 \times 10^{11}$ cm^{-2}). However, the obtained BGR for the $E1$-$H1$ energy gap from the PC analysis must be regarded only as an estimate, since the exact position of the $E1$-$H1^*$ transition is not well defined in the PC spectrum. Nevertheless, the obtained BGR is significantly lower than the -34 meV as estimated from Bauer's calculations[17] and similar values from Schmitt-Rink[18] and Trankle[19] and co-workers for a sample with the parameters of sample 1.

TABLE I. Measured and calculated energies of the strongest transitions in sample 1, and deduced values of BGR.

PC transition	Measured (eV)	Calculated (eV)	Calculated exciton binding energy	Required BGR
$E1$-$H1^*$	~1.545	1.5580		−13.0
$E2$-$H1$	1.562	1.5755	1.3	−12.2
$E2$-$L1$	1.573	1.5877	1.0	−13.7

III. MAGNETOPHOTOCONDUCTIVITY

Photoconductivity spectra were measured as a function of the magnetic field. The signal obtained was highly field dependent, and spectra obtained at some fields were very poor. The reason for this may be understood by considering the contribution of the photoexcited carriers to the resistivity. The number of these carriers is small compared to the total number present, so the dc magnetoresistance is little changed. When the field is such that the Fermi level lies between two Landau levels (or in the localized states), the photoexcited carriers cannot contribute to the photoconductivity, and so the signal is small compared to when the Fermi level lies in the middle of a Landau level. This generates oscillations in the intensity of the PC signal of the same periodicity as the Shubnikov–de Haas oscillations. The phase of the photoconductivity signal also changed with field, which necessitated rephasing the ac detection apparatus for each field.

To improve the resolution, second derivatives of the low-pass filtered photoconductivity spectra were computed and are shown in Fig. 2. Note that in the second derivative some artificial peaks may appear (this is the case for the Moss-Burstein shifted absorption at $B = 0$ T, as can be seen from a comparison of Figs. 1 and 2). The positions of the peaks which could be clearly identified in both the original spectra and the second derivatives are plotted in Fig. 3. Above 5 T, the fan diagram shows that the $E2$-$H1$ magnetoexciton transitions dominate the spectra. In contrast to the $E2$-$H1(1s)$ magnetoexciton,

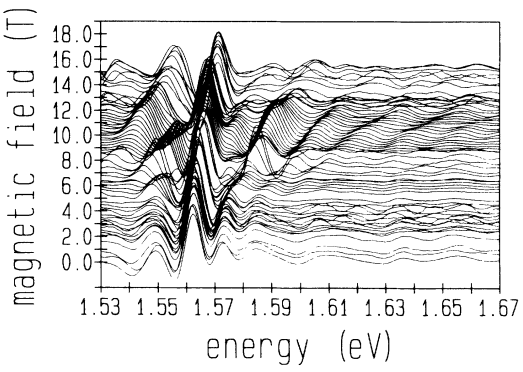

FIG. 2. Second derivative of PC spectra as a function of magnetic field. The B-field value corresponding to each curve is obtained by following the spectrum base line to the scale on the left-hand side.

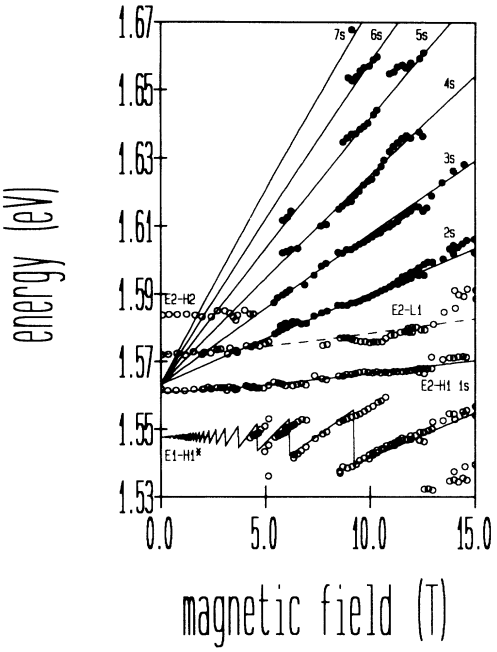

FIG. 3. Plot of the peaks in the PC spectra as a function of magnetic field. Solid lines represent the theoretical fan diagram for the $E2$-$H1$ transitions. The dashed line is the calculated $E1$-$L1(1s)$ magnetoexciton state. The points used in the simultaneous fit of the $E2$-$H1$ Landau-level transitions are depicted by solid circles. The sawtooth curve is the computed position of the Fermi level.

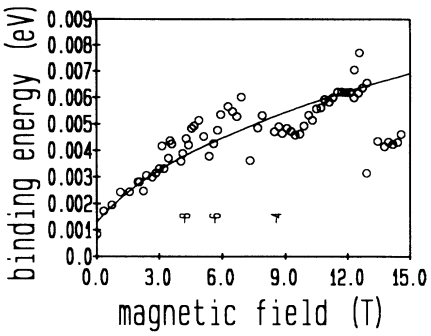

FIG. 4. $E2$-$H1(1s)$ exciton binding as a function of magnetic field. The points represent the difference between the calculated unbound Landau-level transition and the experimental $E2$-$H1(1s)$ energies. The solid line is the theoretical result. The filling factors are also shown by arrows.

which displays a distinct nonlinear diamagnetic shift, the $2s, \ldots, 5s$ transitions were resolved only above 5 T, and in the detected range showed an almost linear dependence on the magnetic field. The theoretical calculations give a vanishing $E2$-$H1(2s)$ binding energy on account of the screening, suggesting that all excited magnetoexcitonic transitions can equally well be described as free-interband Landau-level recombinations. Fitting the magnetic-field dependence of each $E2$-$H1$ Landau-level transition individually, with an in-plane $H1$ mass and a zero-field $E2$-$H1$ free-carrier transition energy as adjustable parameters, gives scattered values, suggesting that these parameters are approximately the same for all Landau-level transitions. The Landau-level transitions in the 5–15-T range were therefore fitted simultaneously, and this is shown in Fig. 3; the solid lines in the figure neglect exciton effects but include nonparabolicity using the method discussed in Ref. 20, with a parameter $K_2 = -1.2$. The deviation of the theoretical fan diagram from the experimental one was found to be very insensitive to a $H1$ hole mass in the range $(0.3-0.7)m_0$. We therefore chose to use a heavy-hole mass in the high-field range of $0.45m_0$, close to the bulk value, which then determines the $E2$-$H1$ continuum edge as 1.5635 meV. The zero-field $E2$-$H1$ binding energy was obtained by subtracting the experimental value for the $E2$-$H1(1s)$ excitonic transition at $B=0$ T from the zero-field $E2$-$H1$ continuum edge energy. This gives a zero-field binding energy of 1.5 ± 0.5 meV, as predicted by the theoretical calculations (see Table I). Thus, the binding energy has been significantly reduced (by screening) from the calculated 7.3 meV in an undoped well.

The exact zero-field $1s$ binding energy is not an accurate absolute value, due to the experimental error, but will provide a self-consistent reference point for the calculation of the field dependence of the binding energy of the $1s$ state, which is defined relative to the $N=0$ free-carrier transition energy, which is only weakly dependent on the heavy-hole mass. The field dependence of the $1s$ binding energy is thus deduced from the difference from the $N=0$ free-carrier transition, and is shown in Fig. 4. This shows an excellent agreement with theory, indicating an almost fivefold increase in binding energy upon application of fields of 15 T. This is much larger than for the unscreened exciton in undoped wells, due to the reduction in the importance in screening as the exciton radius decreases in field. The large $H1$ mass required to fit the excited hole states at high fields is a consequence of the strong nonparabolic valence-band dispersion relations (see, for instance, Ref. 21), and for undoped $GaAs/Al_xGa_{1-x}As$ QW's previous studies have shown that the $H1$ in-plane mass can attain a value as large as $0.85m_0$ at high fields.[22]

IV. MAGNETOLUMINESCENCE

In order to determine the $E1$-$H1$ energy gap with greater precision, the PL spectrum was studied as a function of the applied magnetic field. At zero field no clear transition could be resolved which could be assigned to the $E1$-$H1$ recombination. This occurs due to the overlap of the QW luminescence with the GaAs band-edge PL signal. In addition, a broad emission band with a peak at 1.45 eV was detected in the low-energy side of the PL spectrum, and this emission is attributed to the optical fiber bundle, which was used to conduct the excitation light to the sample, and collect the light emitted by the sample. On applying a magnetic field, the PL signal from the $E1$-$H1$ transition splits into several lines (each corresponding to a different Landau-level recombination), which move rapidly to higher energies, and thus can be conveniently separated from the unwanted emissions (see

Fig. 5). As the intensity of the applied magnetic field is increased, the higher Landau levels are progressively depopulated, the luminescence which they originate weakens, and the luminescence from a given Landau level disappears from the PL spectrum when the energy of such a Landau level becomes larger than the Fermi energy. For instance, at a field of 15 T, only the luminescence from the $N=0$ and $N=1$ Landau levels remain, as shown in Fig. 5; as can be seen, at this field the $N=1$ Landau-level emission is much weaker than the $N=0$ one. This occurs because only a fraction of the $N=1$ Landau level is occupied at 15 T, whereas the $N=0$ Landau level is still fully populated. The overall density of carriers being $n_s=8.2\times10^{11}$ cm^{-2}, of these $2eB/h=7.3\times10^{11}$ cm^{-2} electrons will be in the $N=0$ Landau level at $B=15$ T, and only the remaining 9×10^{10} cm^{-2} in the $N=1$ Landau level, which corresponds to approximately $\frac{1}{10}$ of the total electron density. If the oscillator strength is assumed approximately constant for all Landau-level transitions, then the $N=0$ emission is expected to be 10 times stronger than the $N=1$ one at $B=15$ T.

The peak energies of the emission lines which are attributed to QW luminescence are plotted against magnetic field in Fig. 6. The lines plotted in the fan diagram of Fig. 6 neglect exciton effects, but include nonparabolicity using the method described in Ref. 20, with a nonparabolicity parameter $K_2=-1.2$. The $H1$ hole mass was set to a fixed value of $0.45m_0$, as obtained from the analysis of the magnetophotoconductivity spectra. Thus, the only adjustable parameter is the zero-field transition energy; a value of and 1.511 meV gave the best fit. Independent time-resolved spectroscopic measurements made on this sample at low temperatures also locate the $E1$-$H1$ Γ-point transitions at 1.510 eV.[23] With use of the value of 1.511 eV for the $E1$-$H1$ transition, the corresponding BGR turns out to be -18 meV (see Table I), i.e., larger (by 5 meV) than estimated from the PC experiment. Again, the accuracy of this value is compromised because of the overlapping unwanted luminescence with the quantum-well luminescence in the low-field range.

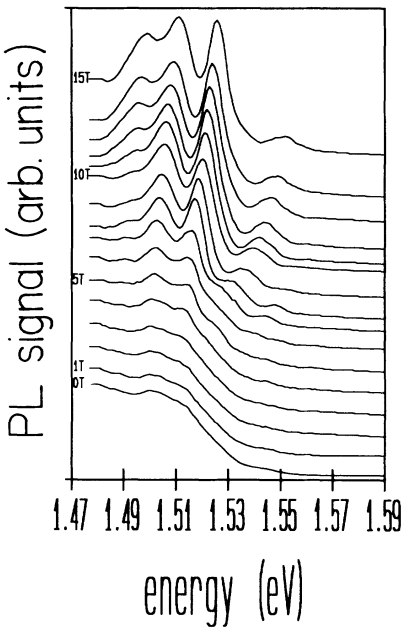

FIG. 5. Photoluminescence spectra at 1-T intervals (field increasing upwards).

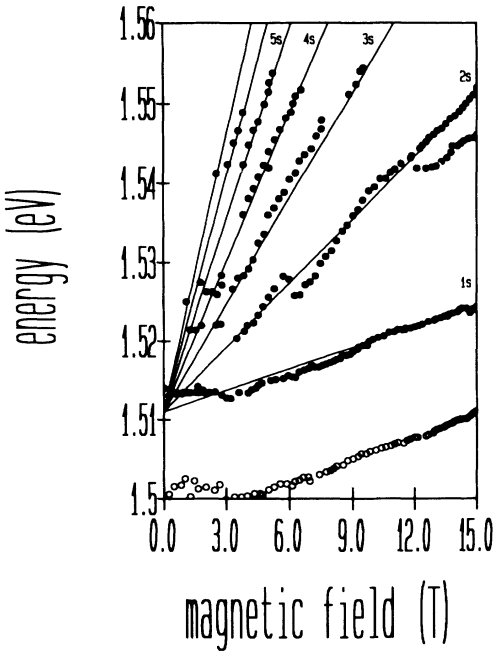

FIG. 6. Plot of transition energies for photoluminescence as a function of applied field. The solid lines correspond to the theoretical model, which includes $E1$ nonparabolicity.

The fan diagram in Fig. 6 has several interesting features. The most important is that exciton effects are absent; notice especially that the $E1$-$H1(N=0)$ branch is not flattened due to excitonic effects. This is to be expected in light of the high carrier density in the fundamental electronic subband. Another feature worthy of comment is the splitting of the $E1$-$H1(N=1)$ transition above 12 T, which can be seen in the spectra of Fig. 5; it is believed that this is due to spin splitting in the valence band, which is, neglecting coupling to other bands, $6\kappa B$ for the $H1$ band, where κ is the parameter that characterizes spin splitting in the valence band. With use of the same value for κ as Ancilotto and co-workers,[21] -1.02, it is found that the splitting should be about 5 meV, in approximate agreement with the observed value. Such a splitting, however, could not be resolved for the other branches of the $E1$-$H1$ transition.

The fan diagram in Fig. 6 also shows, like those of some other authors,[24] oscillations in the transition energy, most noticeably the $2s$ branch. Careful examination of the spectra near 6 T indicate that the corresponding emission intensity seems to undergo a weakening, starting at 5.5 T, but recovers significantly by about 6.5 T, coincidental with the shift in position. Weaker changes in slope can also be distinguished in the $1s$ and $2s$ branches at around 10 T. In samples with two populated subbands, the kinks in the fan diagram and the oscillations in

the luminescence intensity are explained in terms of a field-induced charge exchange between the fundamental and excited electronic subbands, and the consequent effect on the band bending and hence subband-edge energies.[5,3] It is plausible that the magnetodependence of the dielectric function is sufficient to give these kinks;[4] however, the oscillations in the transition energies do not correlate well with the SdH-oscillation minima, as in Ref. 4.

V. CONCLUSION

In summary, our photoconductivity study showed that the $E2$-$H1$ transitions are described by a small but finite binding energy of 1.5 ± 0.5 meV for the $1s$ state, whereas the excited exciton states are not bound due to the screening effect. Under an applied magnetic field, the $E2$-$H1$ binding energy increases very rapidly, due to the changing effects of the screening on the exciton, and its field dependence is very well reproduced by the screened exciton model, which includes the finite thickness of the screening charge. In contrast, photoluminescence showed no evidence of $E1$-$H1$ excitons for a density of 8.2×10^{12} cm^{-2} carriers in the $E1$ subband.

ACKNOWLEDGMENTS

A.B.H. acknowledges support from CNPq, FAPESP, and BID/USP.

[1]S. Schmitt-Rink, D. S. Chemla, and D. A. B. Miller, Adv. Phys. **38**, 89 (1989).

[2]M. S. Skolnick, D. M. Whittaker, P. E. Simmonds, T. A. Fisher, M. K. Saker, J. M. Rorison, R. S. Smith, P. B. Kirby, and C. R. H. White, Phys. Rev. B **43**, 7354 (1991).

[3]J. Orgonasi, J. A. Brum, C. Delalande, G. Bastard, T. Rotger, J. C. Maan, G. Weimann, and W. Schlapp, J. Phys. (Paris) Colloq. **48**, CE-407 (1987).

[4]T. Uenoyama and L. J. Sham, Phys. Rev. B **39**, 11044 (1989).

[5]M. Fritze, W. Chen, and A. V. Nurmikko, in *The Physics of Semiconductors,* edited by E. M. Anastassakis and J. D. Joannopoulos (World Scientific, Singapore, 1990), p. 825.

[6]C. Delalande, G. Bastard, J. Orgonasi, J. Brum, H. Liu, and M. Voos, Phys. Rev. Lett. **59**, 2690 (1987).

[7]R. Stepniewski, M. Potemski, H. Buhmann, D. Toet, W. Knap, A. Raymond, G. Martinez, J. C. Maan, and B. Etienne, in *The Physics of Semiconductors* (Ref. 5), p. 1282; R. Stepniewski, W. Knap, A. Raymond, G. Martinez, J. C. Maan, B. Etienne, and K. Ploog, Surf. Sci. **229**, 519 (1990).

[8]A. B. Henriques, Phys. Rev. B **44**, 3340 (1991); A. B. Henriques, in Proceedings of the IV International Conference on Quantum Well and Superlattice Physics, Somerset (unpublished).

[9]J. Harris, J. Langemaat, S. Battersby, C. Hellon, C. T. Foxon, and D. Lacklison, Semicond. Sci. Technol. **3**, 773 (1988).

[10]G. Wiggins, R. J. Nicholas, J. J. Harris, and C. T. Foxon, Surf. Sci. **229**, 488 (1990).

[11]V. M. Airaksinen, J. J. Harris, D. E. Lacklison, R. B. Beall, D. Hilton, C. T. Foxon, and S. J. Battersby, J. Vac. Sci. Technol. B **6**, 1151 (1988).

[12]A. B. Henriques and E. C. Valadares, Superlatt. Microstruct. **10**, 157 (1991).

[13]X. L. Zheng, D. Heiman, and B. Lax, Phys. Rev. B **40**, 10 523 (1989).

[14]U. Ekemberg and M. Altarelli, Phys. Rev. B **35**, 7485 (1987).

[15]A. Pinczuk, J. Shah, R. Miller, A. Gossard, and W. Wiegmann, Solid State Commun. **50**, 735 (1984).

[16]R. C. Miller, A. C. Gossard, G. D. Sanders, Y. C. Chang, and J. N. Sculman, Phys. Rev. B **32**, 8452 (1985).

[17]G. E. W. Bauer, Surf. Sci. **229**, 374 (1990).

[18]S. Schmitt-Rink and C. Ell, J. Lumin. **30**, 585 (1985).

[19]G. Trankle, H. Leier, A. Forchel, H. Haug, C. Ell, and G. Weimann, Phys. Rev. Lett. **58**, 419 (1988).

[20]D. C. Rogers, J. Singleton, R. J. Nicholas, C. T. Foxon, and K. Woodbridge, Phys. Rev. B **34**, 4002 (1986).

[21]F. Ancilotto, A. Fasolino, and J. C. Maan, Phys. Rev. B **38**, 1788 (1988).

[22]A. Plaut, J. Singleton, R. J. Nicholas, R. Harley, S. Andrews, and C. T. Foxon, Phys. Rev. B **38**, 1323 (1988).

[23]P. Dawson (private communication).

[24]C. H. Perry, J. M. Worlock, M. C. Smith, and A. Petrou, *High Magnetic Fields in Semiconductor Physics,* edited by G. Landwehr, Solid State Science Vol. 71 (Springer-Verlag, Berlin, 1987), p. 202.